The Path of a Growing Crack – A Simulation of the Fracture Process

C. Bjerkén[1] and P. Ståhle[1,2]

[1] Div. Materials Science, Malmö University, Sweden, christina.bjerken@ts.mah.se
[2] Div. Solid Mechanics, Lund University, Sweden, per.stahle@ts.mah.se

ABSTRACT. The growth of a crack subjected to corrosion fatigue is studied using adaptive finite elements. The crack is the image of a deep corrosion pit, and the growth is the result of a repeated cycle of dissolution of the material, formation of a protective oxide film and break-down of the oxide film. The break-down of the film is governed by the strain at the surface and the dissolution rate is assumed to be proportional to this stretching. A threshold strain is assumed to exist below which the oxide film remains intact. With this model, no criterion is needed, neither for crack growth, nor for prediction of the growth direction. The reason is that both are immediate results of the evolution of the body shape. The growth of a semi-infinite crack lying in an infinite strip subjected to different degrees of mixed-mode loading is studied and the results are compared to crack path criteria for sharp cracks. Additionally, the path of a corrosion fatigue crack starting at the surface of an elastic layer attached to a stiff substrate is simulated. The result showed some agreement with experimental results found in the literature.

INTRODUCTION

During stress corrosion, loss of atoms to the environment leads to crack growth. This is a dissolution process that starts if bare metal is exposed to aggressive environments. Fortunately, an impermeable film of mainly metal oxides or hydroxides is formed by dissolved metal. Even though the thickness of this film is typically not more than 10 nm, it reduces the rate of dissolution by several orders of magnitude, cf. [1]. An intact protective film increases the life of the structure tremendously. However, repeated changes of the electrochemical conditions or cyclic mechanical load damage the film, which leads to additional material loss. Several experimental reports show that active loading in terms of either monotonically increasing or fatigue load is an essential prerequisite for development of corrosion cracks, cf. [2]. The passivating film is as being an oxide or hydroxide compound believed to have ceramic material properties. As such it is presumably brittle. Here it is supposed to fracture when stretched more than a threshold strain, ε_f. For strains smaller than ε_f, the film remains intact.

If the threshold strain is exceeded, the film breaks and leave gaps where bare metal is exposed to the environment, see Fig. 1. The area extent of these gaps is assumed to be proportional to the strain exceeding the threshold strain. The broken film leaves gaps that give a discontinuous exposure to environment. To simplify the analysis, the effect is homogenised so that the local dissolution rate is continuously distributed along the body surface. In the present study, the dissolution rate is simply assumed to be proportional to the mechanical stretching of the body surface reduced with the threshold strain.

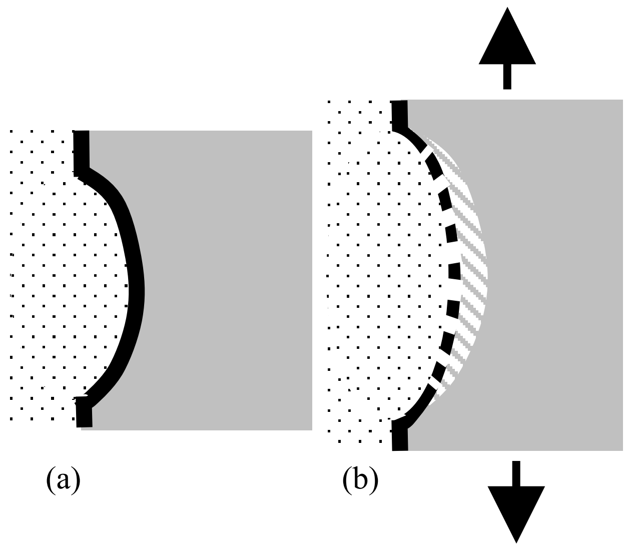

Figure 1. Breakdown of an oxide film (thick black line) on a part of a body (grey area) subjected to a corrosive environment (dotted area). (a) Without mechanical loading; (b) Rupture of film during loading and the consequent dissolution of the material. The dashed area is dissolved and a new surface boundary is formed.

The film is known to be extremely thin as compared with the linear dimensions of the body. Therefore it is not contributing in any significant way to the structural stiffness. In the present analysis, the presence of the film, broken or unbroken, is ignored when the mechanical behaviour of the structure is computed.

The interacting dissolution and mechanical load leads to a roughening of the body surface, and, after localization, to initiation of corrosion pits. For large threshold strains, the pits assume the shape of cracks. These cracks are integral parts of the body surface. Growth rate and growth direction are results of the dissolution process. The model brings additional features to the crack tip in contrast to an assumed sharp crack tip, where the fracture processes are confined to a point and the all details of the crack tip state is given by a single parameter, such as a stress intensity factor or a crack tip driving force. This permits determination of the crack growth simply as the evolution of the body surface. Thus, crack growth criteria are not needed. Neither are crack path criteria needed, while also the direction of the crack extension results from dissolution rate along the body boundaries in the crack tip vicinity.

In the present study, crack paths are calculated using an adaptive finite element procedure. The strain concentration computed from the load and the geometry of the crack tip vicinity predicts dissolution, i.e. removal of material and crack growth. The geometry is repeatedly re-meshed as the body shape is updated to accommodate the extending crack. The mesh maintains a resolution sufficient for a detailed calculation of the strain distribution in the crack tip region to ensure that the crack growth direction is accurately predicted.

Paths are found for a few cases involving different degrees of mixed mode loading. The results are compared with results for established crack path criteria. In addition to this, the path of a crack growing in an elastic layer on a stiff substrate is calculated and compared with an experimental result from the literature.

COMPUTATIONAL METHOD

In the present study, a computational method that evolves a body surface by an adaptive finite element procedure is used, cf. Jivkov [3]. The finite element code ABAQUS [4] is adopted for computing the strains along the surface. During loading, the oxide film is assumed to crack if the strain along the surface exceeds the threshold strain ε_f . This results in dissolution of material. Thus stretching of the body surface controls the rate of dissolution as depicted in Fig. 1. A linear relation between the surface strain ε and the dissolution rate v is assumed:

$$v = C\,(\varepsilon\text{-}\varepsilon_f) \quad \text{for } \varepsilon > \varepsilon_f \qquad (1)$$

where C is a constant depending only on the environment. The rate v is in the present context linear extent per load cycle. The period of the load cycle is assumed to be long enough to allow full recovery of the protective oxide film. The electrochemical potential of the system is contained within C. The surface boundary is moved according to Eq. 1 along the normal direction of the surface. Because of the extremely small thickness of the oxide film, it is not included in the finite element model. Six-node triangular elements are used and re-meshing is done for each load cycle. Further details of the model cf. Jivkov [3]. For both cases studied, the material is assumed linear elastic, and is subjected to fatigue loading under plane strain conditions.

RESULTS

Two different cases are studied. First, simulation of the kinking of a semi-infinite crack in a strip subjected to mixed loading is performed and the results compared with different crack path criteria postulated in the literature. Secondly, the path for a surface crack of elastic layer on stiff substrate is computed and compared to experimental results.

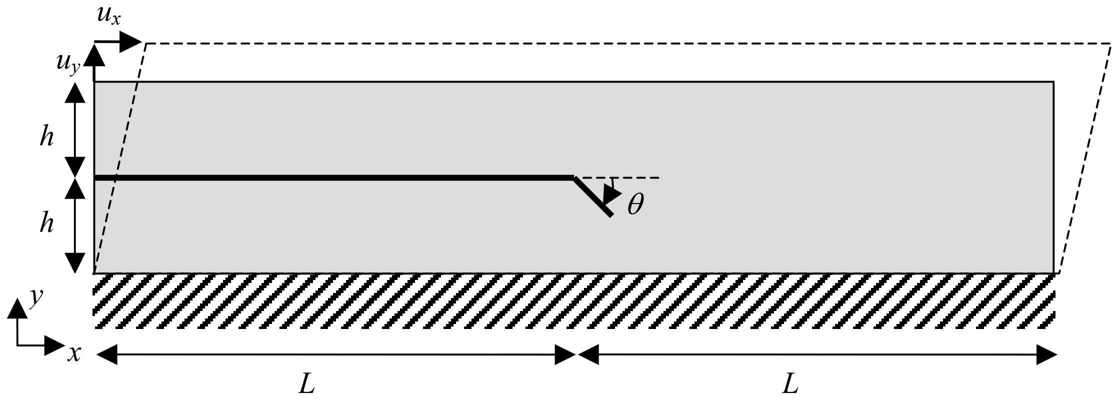

Figure 2. Geometry of the large strip used for the finite element analysis

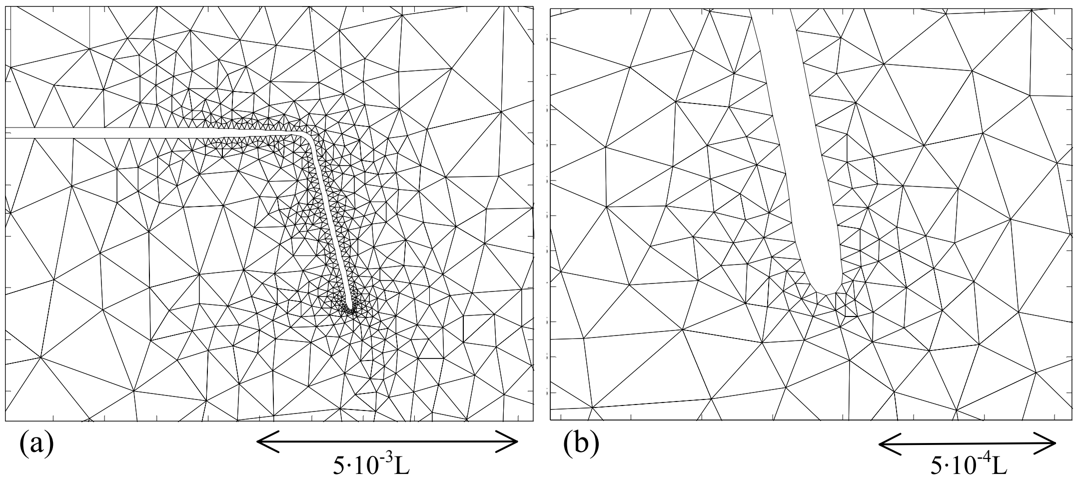

Figure 3. Mesh after 200 load cycles for a strip with global K_{II} load. (a) Area of kink and crack tip; (b) Close-up at the crack tip

Semi-infinite crack in a strip

The crack propagation during is simulated for a semi-infinite crack in a strip, with the initial crack oriented parallel to the surface of the strip, loaded in different degrees of mixed mode. The geometry used for the simulations are shown in Fig. 2. The length of strip is $2L$ and the thickness $2h$, and the lower edge of the strip is allowed to move in the x-direction but is fixed in the y-direction. The load is applied at the upper edge as prescribed displacements u_x and u_y. The lower edge is fixed in both the x- and y-directions. The crack has an initial length L and it is located at $y = h$, between $x = 0$ and L, with its tip at $x = L$. Simulations are performed for a few hundred cycles for eight different degrees of mixed mode loading. In Fig. 3, a typical finite element mesh is shown. Approximately 2000 elements are used during one load cycle, and the ratio of the largest and the smallest element sides is around 4000. The displacement ratio u_x/u_y equals K_{II}/K_I, and the following ratios are investigated: 0, 0.2, 0.5, 1, 2, 5, 10 and ∞.

In Fig. 4, the crack paths after 200 load cycles for the investigated K_{II}/K_I-ratios are shown. The kinked part of a crack is approximately $4 \cdot 10^{-3} L$, the width of the crack is governed by the load and ε_f, cf. [3]. It can be seen that the larger the K_{II}, the more stable the shape of the crack. The crack driven by a global K_I-loading shows a tendency to branch at the crack tip. It can also be noted that for pure K_I global load the present method results in a crack path that is not horizontal initially. Though, after additionally a few hundred cycles this crack will flatten and find a path that is parallel with the initial crack.

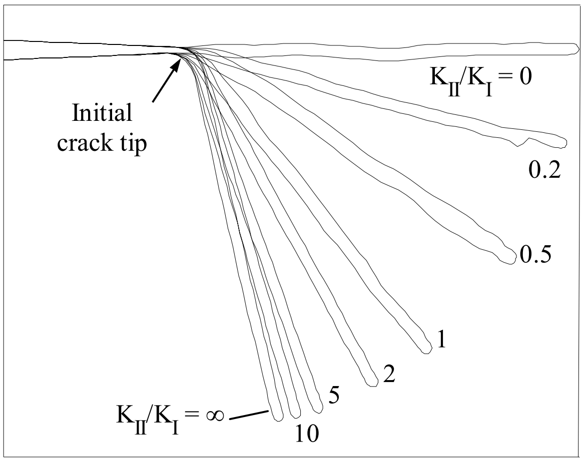

Figure 4. Crack paths for different K_{II}/K_I-ratios

The kink angle, θ, is measured to the centre line of the crack, and the values are plotted in Fig. 5. These results are compared to kink angles obtained by four different crack paths criteria for sharp cracks found in the literature. Melin [5] computed kink angles by maximizing the local mode I stress intensity factor, k_I, at the tip of an infinitesimal kink of a sharp crack. Richard et al. [6] use a criterion based on a numerical adoption to experimental findings. Additionally, two of the criteria studied by Bergqvist and Guex [7] are used for comparison; the criteria of maximum principle stress by Erdogan and Sih [8] (Criterion A) and of the maximum J-integral by Sih [9] (Criterion B). All criteria give similar results as in the present study. For dominating global K_{II} loading, i.e. $K_I=0$, the hypothesis of maximum k_I shows best agreement. In Fig. 5.b, it is seen that at K_I dominance the deviation is larger, with the kink angles found in the present study being smaller than for the criteria of sharp cracks.

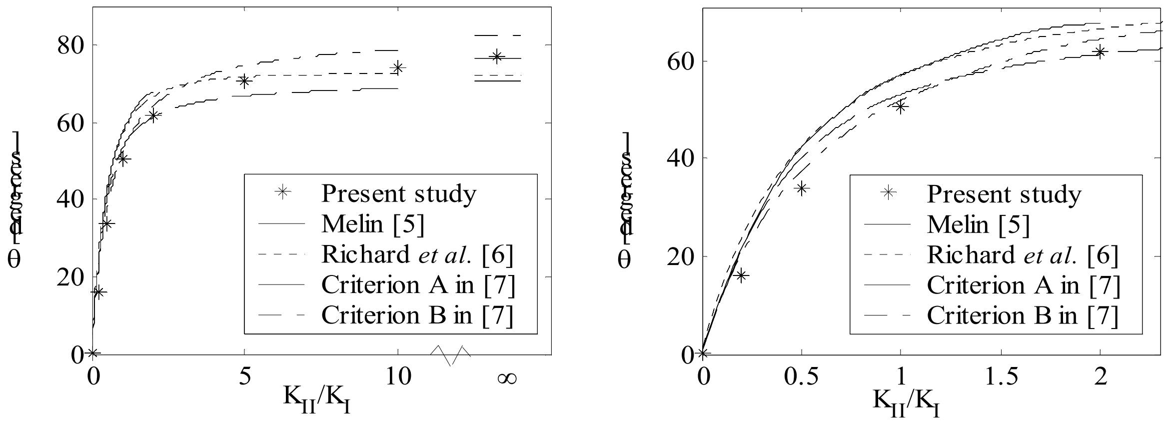

(a) (b)

Figure 5. (a) Kink angles versus K_{II}/K_I for different criteria; (b) Close-up of (a).

Surface crack in an elastic layer on a stiff substrate

The path of a surface crack in an elastic layer attached to a stiff substrate is simulated, see Fig. 6.a. Two opposed point forces, P, are applied at the mouth of an edge crack and the crack is oriented perpendicular to the surface. The thickness of the elastic layer is denoted L and the length of the layer is $2L$. The length of the initial crack is $0.4L$. The geometry of the material and the loading conditions corresponds to those of an experiment performed by Gunnars *et al.* [10]. A weak layer of polycarbonate, with a small initial surface crack of length $0.1L$, was attached to a thick steel bar and the load was applied at the crack mouth by attaching grips connected to a loading device. At the crack tip acetone was dripped which resulted in crack growth due to stress corrosion.
The crack path is shown in Fig. 6.b.

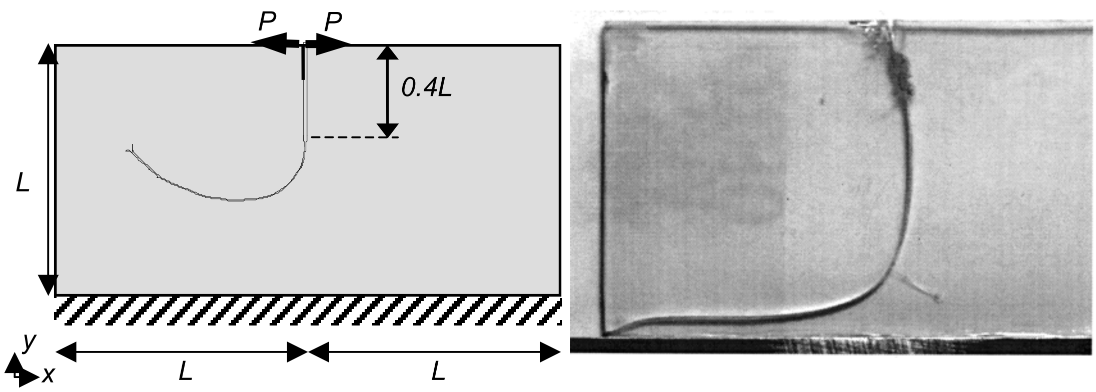

(a) (b)

Figure 6. Comparison between (a) numerical results and (b) results from a stress corrosion experiment of a surface crack in a polycarbonate layer bonded to a steel bar [10].

The simulated crack follows a curved path and avoids the interface and instead it heads towards the stress free surface. It can also be observed that the crack branches at the tip. In a finite element analysis of the stress state at the crack tip for the crack path, found from the experiment, it was concluded that the crack follows a local mode I path, i.e. $K_{II} = 0$, cf. Gunnars *et al*. [10].

DISCUSSION

The present method is based on the calculations of strains along the parts of a body that are in contact with a corrosive media. The tip of the resulting crack has a finite geometry as opposed to conventional methods where it is treated as a single point, cf. Fig. 3.b. The part of the crack tip region that exceeds the threshold strain for oxide film breakage will dissolve and the crack grows by evolving the surface of the body. The presence of T-stresses along the crack flanks will influence the crack growth and may introduce local broadening of the crack tip region which in turn can induce crack branching. Additionally, the crack propagation is sensitive to perturbations arising from the numerical discretisation, and thus proper choices of parameters for the finite element analysis must be made. It is also found that triangular six-node elements give a more stable evolution of the surface than three-node elements.

The comparison of the predicted kink angle showed the largest deviations for nearly horizontal crack growth. It is believed that there is a more pronounced influence of the T-stresses for these cases, thus causing some deviation. The simulations of nearly pure mode I global loading are less stable and the very careful tuning of the settings for the analysis must be performed. While for K_{II} dominance, three-node elements and coarser mesh can be used without loosing accuracy.

A curved crack path and initial branching was obtained in the case of the growth of a surface crack. These features were also found in the experiment [10]. However, in the experiment the crack came closer to the interface the before path changed direction to horizontal growth. The free surface was reached near the interface, which was not the case in the simulations. Plane strain condition is assumed, while in the experiment the elastic layer was a thin polycarbonate. However the width of the crack is very small as compared with the polycarbonate which should give plane strain conditions in the surrounding of the crack tip. Additionally, the location where acetone was applied initially there is evidence of a large area of damaged material which may influence the experimental result. It is believed that the criterion free method can be a plausible choice for studying situations where criteria for crack growth, crack branching and crack path criteria fail, e.g. interface cracks, crack initiation from notch or surface and meeting cracks.

CONCLUSIONS

In the present study, it is shown that crack paths can be followed without criteria for neither crack growth nor crack path. An adaptive finite element procedure was used to simulate the moving boundary of a body subjected to strain driven corrosion fatigue.

Results for kink angles due to mixed mode loading of a crack computed with the presented criteria free method was found to agree well with predictions from criteria for sharp cracks found in the literature. The best agreement was found for dominating global K_{II} loading, while for dominating K_{I} loading the deviation was larger.

A numerical simulation of a surface crack in an elastic material growing towards a stiff substrate demonstrates that the criteria free method can be used to investigate features as crack deviation and branching.

REFERENCES

1. Smallman, R.E. and Bishop, R.J. (1999) *Modern Physical Metallurgy Materials Engineering*, 6th ed, pp. 376-387, Butterworth-Heinemann, Avon, UK.
2. Jones, R.H., and Ricker, R.E. (1992) In: *Stress-Corrosion Cracking*, pp. 1-39, Jones, R.H. (Ed.) ASM International, USA.
3. Jivkov, A. (2002) PhD thesis, Lund University, Sweden
4. ABAQUS/Standard, Hibbit, Karlsson, Sorensen, Inc.
5. Melin, S. (1987) *Int. J. Fract. Mech.* **32**, 257-263.
6. Richard, H.A., Fulland, M. and Sander, M. (2005) *Fatigue Fract. Engng Mater. Struct.* **28**, 3-12.
7. Bergkvist, H. and Guex, L. (1979) *Int. J. Fract.* **15***,* 429-441.
8. Erdogan, F. and Sih, G.C. (1963) *J. Basic Engng*, **85**, 519-527
9. Sih, G.C. (1974) Int. J. Fract., **10**, 305-321.
10. Gunnars, J., Ståhle, P., and Wang, T.C. (1997) *Comp. Mech.* **19**, 545-552.